Millimeter-Wave Communications with Beamforming for UAV-Assisted Railway Monitoring System

Shiyu Su(✉)

School of Electronic and Information Engineering, Beihang University, Beijing 100083, China
1902ssy@buaa.edu.cn

Abstract. Railway is an important means of transportation for passenger and freight, and the maintenance and repair work is essential. Unmanned aerial vehicle (UAV) can be deployed along the railway track for monitoring, reconnaissance and ensuring the safe operation of the railway because of its flexible mobility and low labor cost. In this paper, a railway monitoring system based on aerial platform is formed, which takes UAV monitoring as the main body. In order to solve the problem of long-distance and wide bandwidth backhaul communication, this paper adopts mmWave array communication scheme, and designs the large antenna array beamforming on the base station receiver with zero-forcing (ZF) and minimum mean square error (MMSE). Finally, the simulation results show that the minimum mean square error method is effective, and the simulation results also provide a reference for the UAV deployment along the railway.

Keywords: UAV · Beamforming · ZF · MMSE · Railway monitoring · Uplink transmission

1 Introduction

As an important transportation system, the railway's daily stable operation determines the normal operation of national production and life. In order to ensure the track components are in good condition, the railway line must be monitored, regularly inspected and maintained. At present, manual inspection is the most common method of railway line maintenance. The patrol officer uploads the railroad track picture, the latitude and longitude coordinates through the terminal installed on the mobile phone [1]. However, such a line-traveling process is time-consuming and labor-intensive.

This work was supported in part by the National Key Research and Development Program (Grant Nos. 2016YFB1200100), and the National Natural Science Foundation of China (NSFC) (Grant Nos. 61827901 and 91738301).

B. Li et al. (Eds.): IoTaaS 2020, LNICST 346, pp. 721–731, 2021.
https://doi.org/10.1007/978-3-030-67514-1_57

With the reform of the operation system, the railway development should take quality first and efficiency first as the measurement standard [2]. Therefore, the railway patrol inspection requires limited manpower and advanced technical means to fully control the situation along the railway. Combining image monitoring, GPRS wireless communication and automatic control technology, reference [3] actualised the monitoring and data transmission of railway crossing. However, it's well known that the coverage of outdoor cameras is so small that it is impossible to monitor the entire railway from the ground. The authors in [4] introduced the research and development overview of East Japan Railway's line detection device, and put forward a monitoring method of installing inspection devices on trains. However, the applicable speed of the device is below 120 km/h. Inspired by the previous works, this paper proposes a railway surveillance system based on an aerial platform, where multiple unmanned aerial vehicles (UAVs) simultaneously patrol along the railway line, uploading image data to a high-altitude airship in real time.

In recent years, the UAV industry has developed rapidly. Thanks to its flexible mobility and low labor cost, UAVs are widely used in various fields such as communications, reconnaissance, surveillance, remote sensing, aerial photography, disaster relief, and agricultural irrigation [5,6]. Compared with the ground monitoring, the air-based railway monitoring system has a more flexible inspection mode, but it still needs to solve the problem of wide bandwidth backhaul. Due to the need to monitor the entire railway, there are many pictures and large amounts of data. But the bandwidth requirements cannot be met in the sub-6G frequency band. In order to alleviate the shortage of low-band spectrum and further improve the system's communication and monitoring capabilities, one of the most effective ways is to use the Millimeter-Wave band [7]. Compared with current cellular band (3G or LTE) signals, mmWave signals will experience severe path loss, penetration loss and rain attenuation [8]. Therefore, it is necessary to use a large-scale array antenna to perform beamforming on the receiving end of the airship to obtain a beam pointing to the UAV along the railway. At the same time, in the mmWave band, shorter wavelengths enable more antennas to be compressed in the same size, thus allowing large-scale spatial multiplexing and high directional beamforming.

At present, there have been some studies on beamforming of microwave band systems. The authors in [9] proposed a three-dimensional beamforming algorithm applied to the downlink multi-input multi-output (MIMO) system, which performed multi-user grouping and inter-user interference suppression. In [10], the author proposed a three-dimensional beamforming strategy based on area division to ensure that all users can obtain a fair beam gain. The authors in [11] studied the design of hybrid beamforming in the mmWave MU-MIMO system of high-speed railways. And a two-stage algorithm of hybrid beamforming at transmitter and receiver was proposed, which could still have high total throughput in mmWave channel with time delay and doppler effect.

In this paper, the uplink transmission scenario of UAVs is established, and two commonly used beamforming algorithms of different microwave band

systems are compared. Besides, the application of the better scheme is extended to provide reference for UAV detection deployment along the railway. The remainder of this paper is organized as follows. The system model is described in Sect. 2. Hybrid beamforming designs are elaborated in Sect. 3. Section 4 presents the simulation results. Section 5 concludes this paper and discusses the deployment of UAVs.

Notation: a, $\mathbf{a}$, $\mathbf{A}$ and $\mathcal{A}$ denote a scalar, a vector, a matrix and a set, respectively. $\|\mathbf{a}\|$ denotes the Frobenius norm of $\mathbf{a}$. $[\mathbf{A}]_{i,j}$ denotes the entry in the i-th row and j-th column of matrix $\mathbf{A}$.

2 System Model

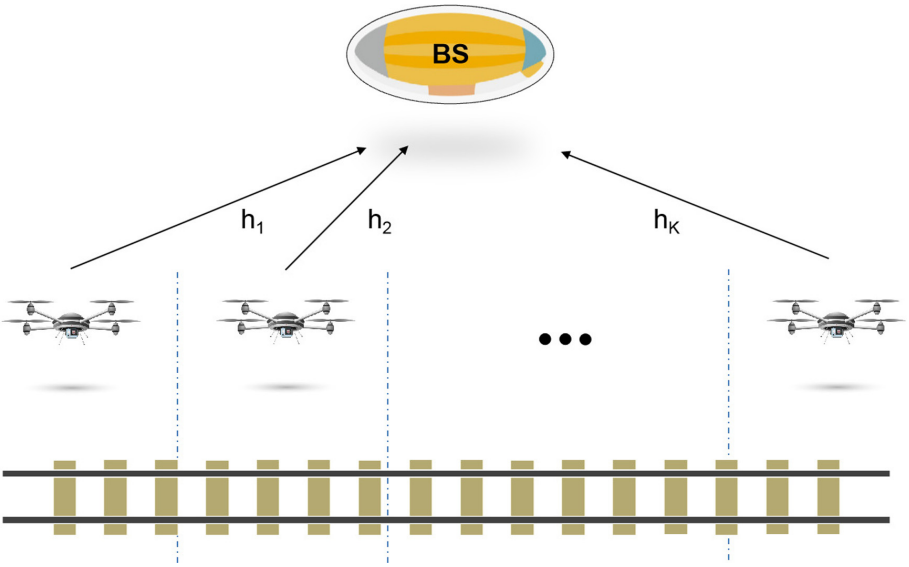

Fig. 1. Scene along the railway.

The schematic diagram of the scene along the railway is shown in Fig. 1. In a section of the railway line with a total length of L, there are K tethered drones, and an airship is used as a base station (BS) above the middle section of the railway. The airship equipped with large-scale antenna arrays, needs to serve the UAV group in the target area. The flying height difference between the airship and UAVs is h, and the number of antennas is N. The channel between the user and the BS is regarded as a millimeter wave channel with spatial sparsity. Since the occlusion and scattering in the link are relatively weak, the line-of-sight(LOS) transmission path is significantly stronger than the non-line-of-sight (NLOS) transmission path [12]. Because ground obstacles will

seriously affect the line-of-sight transmission path, the receiving end does not use ground base stations but high-airships. Due to the limited scattering in the mmWave band, the multipath is mainly caused by reflection. Since the number of multipath components is usually small, the mmWave channel has directivity and spatial sparsity occurs in the angle domain. Different multipath components have different angles of arrival. Without loss of generality, we use the directional mmWave channel model, then the channel between each UAV and the base station can be expressed as [13,14]:

$$\mathbf{h}_i = \sum_{\ell=1}^{L_i} \lambda_{i,\ell} \mathbf{a}\left(N, \Omega_{i,\ell}\right) \tag{1}$$

where λ is the channel gain complex coefficient of the transmission path, Ω is the cosine of the pitch angle of the line-of-sight transmission path, and the subscripts i and l represent the l-th multipath of the i-th UAV. L_i represents the total multipath number of the i-th UAV, which includes one LOS path and $L_i - 1$ NLOS path. $\mathbf{a}(\bullet)$ refers to a vector function, which is defined as:

$$\mathbf{a}(N, \Omega) = \left[e^{j\pi 0\Omega}, e^{j\pi 1\Omega}, e^{j\pi 2\Omega}, \cdots, e^{j\pi(N-1)\Omega}\right]^T \tag{2}$$

The system model is shown in Fig. 2. Each UAV has a single antenna and sends signals to the airship with power $\mathbf{P}$.The airship's receiver has N antennas, and each antenna is connected to K phase converters to form the front-end analog beamforming. Behind the analog beamforming, there are K RF chains (equal to the number of users). Each RF chain receives signals from all antennas. Finally, after digital beamforming, the received signal $\mathbf{y}$ is obtained. So the expression of the received signal can be written as:

$$\mathbf{y} = \mathbf{D}^H \mathbf{A}^H \left[\mathbf{HPs} + \mathbf{z}\right] \tag{3}$$

where, $\mathbf{H} = [\mathbf{h}_1, \ldots, \mathbf{h}_K]$ is the channel matrix, $\mathbf{s} = [s_1, \ldots, s_K]^T$ is the data of K UAVs, and $\mathbf{z}$ is the Gaussian white noise. $\mathbf{A}$ is $N \times K$ matrix, representing analog beamforming; $\mathbf{D}$ is $K \times K$ matrix, representing digital beamforming. $\mathbf{P}$ is a diagonal matrix, and the transmission power of each UAV is on the diagonal of it, i.e,

$$\mathbf{P} = \begin{pmatrix} p_1 & & 0 \\ & \ddots & \\ 0 & & p_K \end{pmatrix} \tag{4}$$

After obtaining the expression of the received signal, the achievable rate of the k-th UAV can be calculated according to the Shannon formula:

$$R_k = \log_2(1 + SINR_k) \tag{5}$$

where,

$$SINR_k = \frac{\left|\mathbf{d}_k^H \mathbf{A}^H \mathbf{h}_k\right|^2 P}{\sum\limits_{j \neq k} \left|\mathbf{d}_j^H \mathbf{A}^H \mathbf{h}_j\right|^2 P + \left\|\mathbf{D}^H \mathbf{A}^H\right\|_2^2 \delta^2} \tag{6}$$

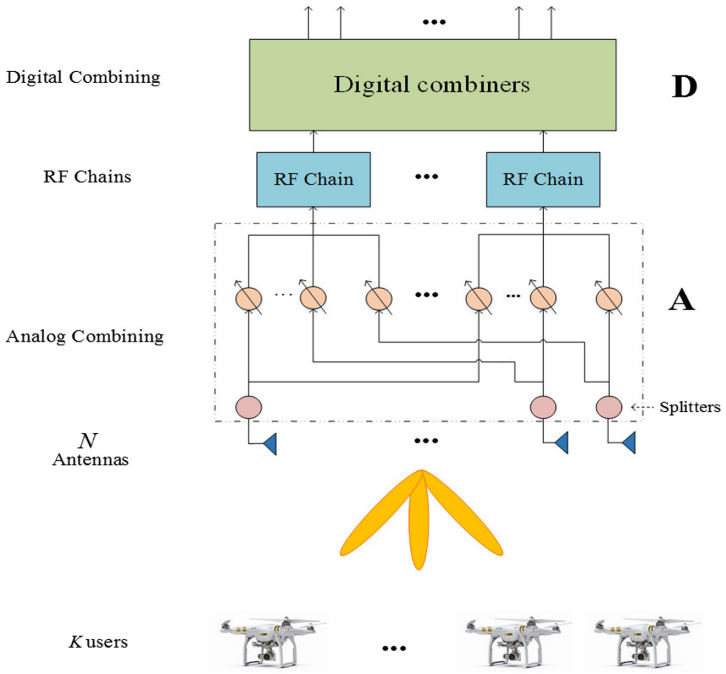

Fig. 2. System model.

Therefore, the problem of this scenario is using beamforming to design two appropriate matrices of **A** and **D**, so that the sum of the achievable rate of the UAVs is maximized. In order to increase the array gain of the analog domain, the analog beamforming should match the channel. Therefore, the phase of each column of the **A** matrix is the corresponding phase of each UAV channel, which is shown with formula (7). The commonly used beamforming algorithms are zero forcing (ZF) and minimum mean square error (MMSE). Next, we will use these two methods to calculate **D**, and compare their performance through simulation.

$$[\mathbf{A}]_{i,j} = \frac{[\mathbf{H}]_{i,j}}{\left|[\mathbf{H}]_{i,j}\right|} \tag{7}$$

3 Hybrid Beamforming

3.1 ZF Beamforming Design

The zero-forcing (ZF) algorithm is the most basic and simplest algorithm in linear precoding. Under the premise of knowing the channel matrix, it can eliminate the interference between multiple channels [15]. Since this paper is directed to the **D** matrix for zero-forcing beamforming, the **A** matrix at the front end

needs to be considered as part of the channel matrix. Therefore, the part before digital beamforming is regarded as an equivalent channel $\mathbf{H}_{eff}$:

$$\mathbf{H}_{eff} = \mathbf{A}^H \mathbf{H} \tag{8}$$

$$\mathbf{y} = \mathbf{D}^H \mathbf{H}_{eff} \mathbf{P} \mathbf{s} + \mathbf{D}^H \mathbf{A}^H \mathbf{z} \tag{9}$$

After obtaining the equivalent channel, Eq. (3) can be rewritten as shown in Eq. (9). Assuming a feasible matrix $\tilde{\mathbf{D}}$, defined by the zero-forcing method, the $\tilde{\mathbf{D}}$ matrix should satisfy:

$$\tilde{\mathbf{D}}^H \mathbf{H}_{eff} = \begin{pmatrix} x_1 & & 0 \\ & \ddots & \\ 0 & & x_K \end{pmatrix} \tag{10}$$

In this way, the coefficient matrix of the previous term of Eq. (9) is a diagonal matrix, thereby eliminating interference between UAVs. Where x_1, x_2, ..., x_K are real coefficients. Then by observing Eq. (6), we can find that when calculating the achievable rate of each UAV, the diagonal coefficients of Eq. (10) are cancelled, so the conjugate transpose of $\tilde{\mathbf{D}}$ can be directly equal to the inverse matrix of $\mathbf{H}_{eff}$. And the expressions of the received signal and the UAV achievable rate are rewritten as follows:

$$\mathbf{y} = \mathbf{P}\mathbf{s} + \tilde{\mathbf{D}}^H \mathbf{A}^H \mathbf{z} \tag{11}$$

$$SINR_k = \frac{P}{\left\| \tilde{\mathbf{D}}^H \mathbf{A}^H \right\|_2^2 \delta^2} \tag{12}$$

3.2 MMSE Beamforming Design

The basic principle of beamforming technology based on the minimum mean square error (MMSE) criterion is consistent with MMSE precoding [16]. It is a algorithm to make the received data as close as possible to the transmitted data. This method can Effectively ensure the fairness of each user. Therefore, the purpose of MMSE is to find a matrix $\mathbf{D}$ to make $\mathbf{y}$ closer to $\mathbf{s}$. According to the definition, we take the difference between the received signal and the transmitted signal and take the average value, which can be obtained from Eq. (9):

$$E[\left\| \tilde{\mathbf{D}}^H (\mathbf{H}_{eff} \mathbf{P} \mathbf{s} + \mathbf{A}^H \mathbf{z}) - \mathbf{s} \right\|_2^2] \tag{13}$$

If the minimum value of the above formula is required, the $\mathbf{D}$ matrix needs to be derived first, and then the derivative function is zero to obtain the solution of the $\mathbf{D}$ matrix. Here, assuming that the transmission power of each UAV is equal and all are $\mathbf{P}$, derivation of Eq. (13) can be obtained (see appendix for specific derivation):

$$\begin{aligned} \tilde{\mathbf{D}} &= \sqrt{P} \mathbf{J}^{-1} \mathbf{H}_{eff} \\ where, \mathbf{J} &= (P \mathbf{H}_{eff} {\mathbf{H}_{eff}}^H + \delta^2 \mathbf{A}^H \mathbf{A}) \end{aligned} \tag{14}$$

4 Simulations

In the simulation, we use the channel model as shown in formula (1). The amplitude of the complex coefficient $\lambda_{i,\ell}$ of the Los channel gain is inversely proportional to the distance, and the average strength of $\lambda_{i,\ell}$ is set to be 1 when the distance between the airship and the UAV is 20 km. In addition, it is assumed that there are four NLOS paths, and each complex coefficient is generated by Gaussian random function, but the gain is 20 dB smaller than that of Los path. The height difference h between UAV and airship is 20 km, the total number k of UAV is 5, and the total length L of UAV reconnaissance track is 100 km. The simulation results of the two methods are as follows:

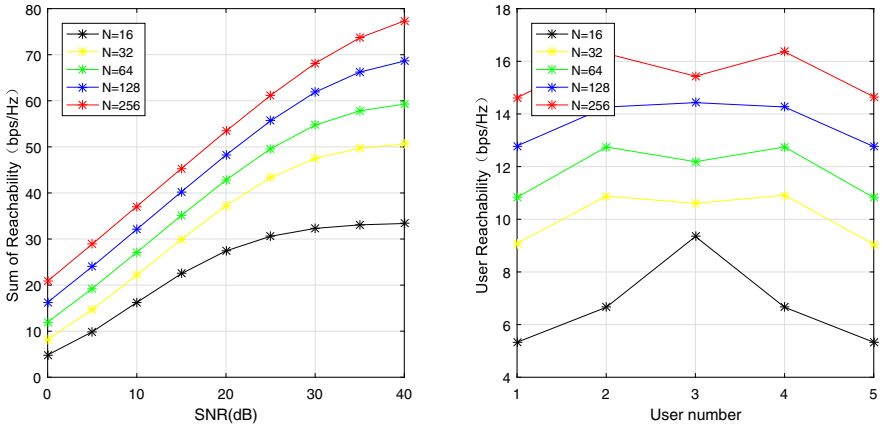

(a) achievable rate curve. (b) Comparison of UAV achievable rate.

Fig. 3. Simulation results of beamforming with ZF algorithm.

Overall comparison of Fig. 3 and Fig. 4 shows that the beamforming designed by the MMSE algorithm is superior to the ZF algorithm. The simulation results of the MMSE show almost five parallel lines. Both the increase in the number of antennas and the increase in SNR can significantly improve the reachability. The curves of the ZF method are more sparse than the former. As the number of antennas increases, the reachability does not increase linearly. And as the SNR rises, the curve also tends to slow down, indicating that the ZF algorithm may appear saturated at high signal-to-noise ratios. The figure on the right shows the reachability curve of each UAV with an SNR of 40 dB. It can be seen in Fig. 4 that the achievable rate is a straight horizontal line regardless of the number of antennas. It shows that the MMSE algorithm makes the achievable rate of each UAV almost equal, which can ensure the fairness of each UAV. This is because the MMSE method pursues the smallest error between the received signal and the transmitted signal, regardless of the location of the UAV. And the fairness

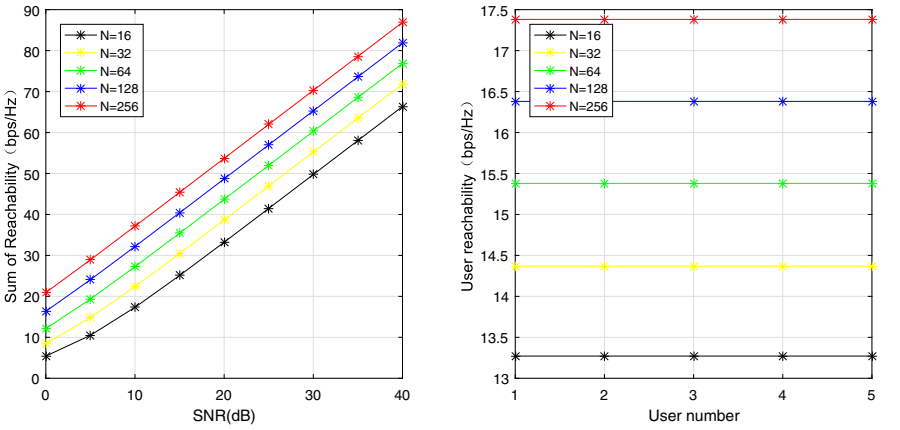

(a) achievable rate curve. (b) Comparison of UAV achievable rate.

Fig. 4. Simulation results of beamforming with MMSE algorithm.

under this beamforming can just ensure that the UAV inspection at any position will not affect its uplink transmission.

In general, the zero-forcing method has low complexity and simple implementation. Although it can eliminate the interference between multiple signals, it ignores the influence of noise during the operation, resulting in a decrease in the reachability. The MMSE beamforming method is fair and can be well adapted to the space-based platform monitoring system.

In addition, on the basis of adopting the MMSE algorithm, this paper also explores the optimal number of UAVs. Figure 5 shows the effect of the number of UAVs on the total efficiency rate on a fixed-length railway line. It can be seen from the figure that the more UAVs deployed, the more information can be transmitted. But more UAVs mean more energy consumption and RF link requirements. Figure 6 shows the influence of the number of UAVs on energy effectiveness. Energy effectiveness is the ratio of total power consumption and total achievable rate, where the total power consumption includes the power of the receiver on the base station, and the power of all antennas and phase converters.

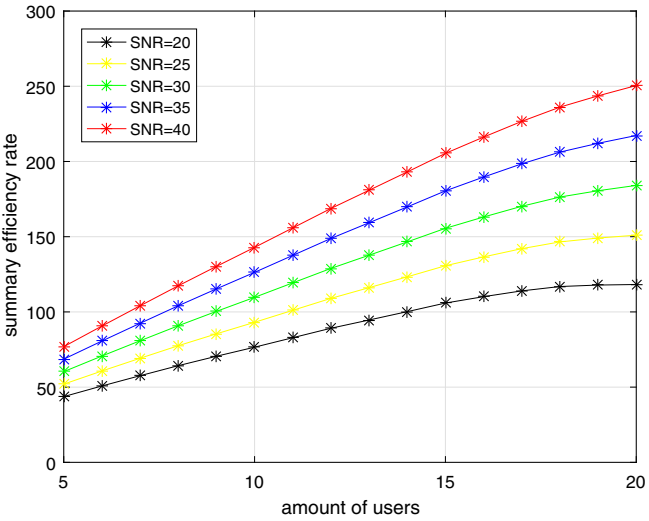

Fig. 5. Influence of UAV number on summary efficiency rate (MMSE).

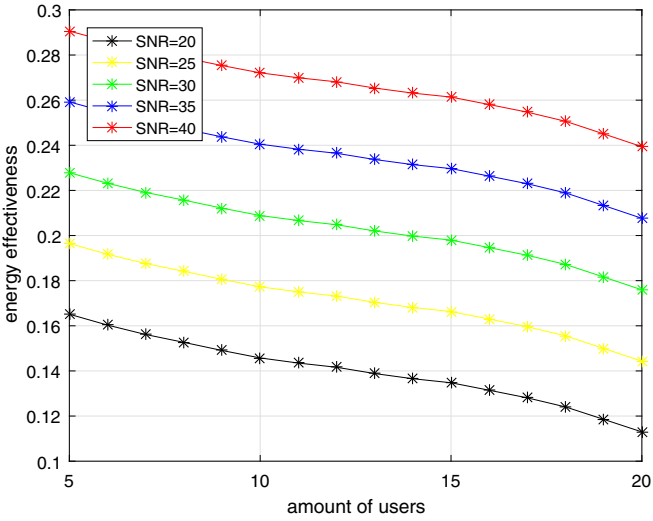

Fig. 6. Influence of UAV number on energy effectiveness (MMSE).

5 Conclusions

This paper proposed a railway monitoring system based on an air-based platform. An uplink transmission scenario for railway UAV inspection was established, and beamforming was designed at the receiving end of the system. The digital beamforming matrix was calculated using the zero forcing algorithm and

MMSE algorithm, and the transmission performance of the two methods were compared through simulation. The simulation results showed that the beamforming designed by the MMSE could achieve a higher achievable rate, and at the same time, it could well guarantee fairness. Simulation results show that with the increase of UAVs, it could ensure that the information transmission capacity increases steadily. However, too many UAVs reduce the overall energy efficiency, so the number of UAVs needs to be determined based on the speed of the UAV inspection and the length of the railway.

Appendix

Equation (14) derives the $\tilde{\mathbf{D}}$ matrix as follows. First, convert Eq. (14) to expression:

$$f(\tilde{\mathbf{D}}) = Tr\{E[(\tilde{\mathbf{D}}^H \mathbf{H}_{eff}\mathbf{P}\mathbf{s} + \tilde{\mathbf{D}}^H \mathbf{A}^H \mathbf{z} - \mathbf{s})(\mathbf{s}^H \mathbf{P}{\mathbf{H}_{eff}}^H \tilde{\mathbf{D}} + \mathbf{z}^H \mathbf{A}\tilde{\mathbf{D}} - \mathbf{s}^H)]\} \quad (15)$$

Then expand the above formula and simplify:

$$f(\tilde{\mathbf{D}}) = Tr(P\tilde{\mathbf{D}}^H \mathbf{H}_{eff}{\mathbf{H}_{eff}}^H \tilde{\mathbf{D}} - \tilde{\mathbf{D}}^H \mathbf{H}_{eff}\mathbf{P} + \delta^2 \tilde{\mathbf{D}}^H \mathbf{A}^H \mathbf{A}\tilde{\mathbf{D}} - \mathbf{P}{\mathbf{H}_{eff}}^H \tilde{\mathbf{D}} + \mathbf{I}) \quad (16)$$

Derivative the above formula to $\tilde{\mathbf{D}}$ and make it equal to zero

$$\frac{df}{d(\tilde{\mathbf{D}}^H)} = P\tilde{\mathbf{D}}^T {\mathbf{H}_{eff}}^* {\mathbf{H}_{eff}}^T - \sqrt{P}{\mathbf{H}_{eff}}^T + \delta^2 \tilde{\mathbf{D}}^T \mathbf{A}^T \mathbf{A}^* = 0 \quad (17)$$

$$\Rightarrow \tilde{\mathbf{D}}^T (P{\mathbf{H}_{eff}}^* {\mathbf{H}_{eff}}^T + \delta^2 \mathbf{A}^T \mathbf{A}^*) - \sqrt{P}{\mathbf{H}_{eff}}^T = 0 \quad (18)$$

$$\begin{gathered} \therefore \tilde{\mathbf{D}} = \sqrt{P}\mathbf{J}^{-1}\mathbf{H}_{eff} \\ where, \mathbf{J} = (P\mathbf{H}_{eff}{\mathbf{H}_{eff}}^H + \delta^2 \mathbf{A}^H \mathbf{A}) \end{gathered} \quad (19)$$

References

1. Jiang, W.: On railway comprehensive inspection and safety management. Technol. Startup Mon. **024**(17), 146–148 (2011)
2. Huang, M.: Reflection on railway development and reform in the new era. China Railw. Corp. **041**(006), 1–8 (2019)
3. Sun, J., Song, H., Zhou, Y.: Using wireless communication to monitor railway crossings. Railw.Tech. Superv. **1**, 48–50 (2010)
4. Ryo, T.: (Japan): monitoring technique for track conditions of east japan railway. JR-EAST **053**(1), 35–40 (2016)
5. Xiao, Z., Xia, P., Xia, X.G.: Enabling UAV cellular with millimeter-wave communication: Potentials and approaches. IEEE Commun. Mag. **54**(5), 66–73 (2016)

6. Jian, W., Gao, F., Wu, Q., Shi, J., Yi, W., Jia, W.: Beam tracking for UAV mounted SatCom on-the-move with massive antenna array (2017)
7. Cui, Y., Fang, X., Fang, Y., Xiao, M.: Optimal non-uniform steady mmWave beamforming for high speed railway. IEEE Trans. Veh. Technol. **67**, 4350–4358 (2018)
8. Haider, F.: Cellular architecture and key technologies for 5G wireless communication networks. J. Chongqing Univ. Posts Telecommun. **52**(2), 122–130 (2014)
9. Li, X., Jin, S., Suraweera, H.A., Hou, J., Gao, X.: Statistical 3-D beamforming for large-scale MIMO downlink systems over Rician fading channels. IEEE Trans. Commun. **64**(4), 1529–1543 (2016)
10. Zhang, Z., Chan, K., KwokHung, L.: Study of 3D beamforming strategies in cellular networks with clustered user distribution. IEEE Trans. Veh. Technol. **65**, 10208–10213 (2016)
11. Gao, M., Bo, A., Niu, Y., Zhang, Z., Li, D.: Dynamic mmWave beam tracking for high speed railway communications. In 2018 IEEE Wireless Communications and Networking Conference Workshops (WCNCW) (2018)
12. Xiao, Z., Zhu, L., Choi, J., Xia, P.: Joint power allocation and beamforming for non-orthogonal multiple access (NOMA) in 5G millimeter-wave communications. IEEE Trans. Wirel. Commun. **17**, 2961–2974 (2018)
13. Ding, Z., Fan, P.: Impact of user pairing on 5G nonorthogonal multiple-access downlink transmissions. IEEE Trans. Veh. Technol. **65**(8), 6010–6023 (2016)
14. Xiao, Z., Xia, P., Xia, X.G.: Codebook design for millimeter-wave channel estimation with hybrid precoding structure. IEEE Trans. Wirel. Commun. **16**(1), 141–153 (2016)
15. Taesang, Y., Goldsmith, A.: On the optimality of multiantenna broadcast scheduling using zero-forcing beamforming. IEEE J. Sel. Area Commun. **24**(3), 528–541 (2006)
16. Bahrami, H.R., Le-Ngoc, T.: MMSE-based MIMO precoder using partial channel information. In: IEEE International Conference on Wireless and Mobile Computing, Networking and Communications, 2005. (WiMob'2005) (2005)